

Backstepping nonlinear control of a five-phase PMSG aerogenerator linked to a Vienna rectifier

Adil Mansouri, Abdelmounime El Magri, Ilyass El Myasse, Rachid Lajouad, Nabil Elaadouli

EEIS Laboratory, ENSET Mohammedia, Hassan II University of Casablanca, Casablanca, Morocco

Article Info

Article history:

Received Jun 15, 2023

Revised Jul 22, 2023

Accepted Jul 27, 2023

Keywords:

Artificial neural network

Backstepping control

Five-phase PMSG

Maximum power point tracking

Renewable energy systems

ABSTRACT

The objective of this study is to create a nonlinear control system designed for a Vienna converter-connected five-phase aerogenerator. The control strategy will be based on the space vector pulse width modulation (SVPWM) technique, which is more suitable for controlling rectifier switches. Due to the higher complexity of the five-phase permanent magnet synchronous generator (PMSG) machine than the conventional three-phase generator, it poses a difficult control problem requiring an advanced mathematical model. Integrating an aerogenerator with a Vienna converter enhances efficiency and power quality. The primary purpose of this study is to develop a nonlinear controller utilizing the retrogression control strategy alongside the SVPWM approach. Furthermore, a speed optimizer based on an artificial neural network is implemented to improve the system's overall efficiency and meet multiple objectives. The proposed control system improves the overall operation and efficiency of Vienna's integrated wind turbine and rectifier system.

This is an open access article under the [CC BY-SA](https://creativecommons.org/licenses/by-sa/4.0/) license.



Corresponding Author:

Adil Mansouri

EEIS Laboratory, ENSET Mohammedia Hassan II University of Casablanca

Casablanca, Morocco

Email: mansouri_adil@yahoo.com

1. INTRODUCTION

Permanent magnet synchronous generators are widely used in wind turbines to convert wind energy into electrical power. The use of five-phase generators offers improved fault tolerance and reliability [1], [2]. Compared to three-phase generators, when one of the windings or phases fails, the remaining four phases can continue to generate electricity, and the windings in the permanent magnet synchronous generator (PMSG) result in smoother and more constant power output. This is particularly beneficial in wind power applications, as wind speed fluctuations can lead to output power variations in three-phase generators. The five-phase configuration reduces the impact of wind gusts and helps maintain a more stable electrical output. The Vienna rectifier has gained recognition for its exceptional attributes, including high power factor, low harmonic distortion (THD), and high efficiency, particularly when operated under space vector pulse width modulation (SVPWM). The SVPWM provides an improved power output with less electromagnetic noise. In their comparative study [3], Hussein and Mohammed found that SVPWM exhibits the lowest THD among various pulse width modulation (PWM) techniques, indicating its superiority in reducing distortion and improving power quality. Another study, [4] reviewed different SVPWM methods and their applications in multilevel inverters and concluded that SVPWM proves to be the most efficient method for minimizing harmonic distortion and improving the output power quality.

A plethora of nonlinear controllers have been explored in the existing literature [5]–[8]. Backstepping control is a nonlinear control technique that has undergone extensive research and practical implementation in diverse systems. It offers a systematic methodology for controller design involving the recursive construction of Lyapunov functions to stabilize the system dynamics. Backstepping control provides several advantages, including robustness and precise control, especially for systems characterized by nonlinearities and uncertainties [9]–[11]. To design the controller, the reference speed is provided by an artificial neural network (ANN) algorithm generated using only electrical measurements. This method is quite effective, outperforming traditional methods and yielding superior performance [12]–[15]. The paper is structured in the following manner: it starts with the introduction, then the system modeling in section 2. Section 3 covers the controller design, while section 4 details the simulation procedure and presents the results. Finally, the conclusion will conclude the study.

2. SYSTEM MODELING

The five-phase aerogenerator-based PMSG mathematical model is stated as shown in previous studies [16]–[18] as (1)–(5).

$$J \frac{d\Omega}{dt} = -F\Omega + K_M i_{sq} - T_g \quad (1)$$

$$L_s \frac{di_{sq}}{dt} = -R_s i_{sq} - p L_s i_{sd} \Omega - \frac{2}{5} K_M \Omega + v_{sq} \quad (2)$$

$$L_s \frac{di_{sd}}{dt} = -R_s i_{sd} + p i_{sq} \Omega + v_{sd} \quad (3)$$

$$L_s \frac{di_{sx}}{dt} = -R_s i_{sx} + v_{sx} \quad (4)$$

$$L_s \frac{di_{sy}}{dt} = -R_s i_{sy} + v_{sy} \quad (5)$$

In dq-coordinates, the stator current and voltage are denoted by (i_{sd}, i_{sq}) and (v_{sd}, v_{dq}) , respectively. Similarly, the xy-coordinate projections of stator current and voltage are represented by (i_{sx}, i_{sy}) and (v_{sx}, v_{dy}) . The viscosity coefficient is indicated as F , whereas rotor inertia and rotor speed are denoted as J and Ω , respectively. Additionally, p signifies the pole pair number, T_g represents the input torque, and the flux generator parameter is represented by K_M . Finally, the whole model of the proposed structure in Figure 1, referring to [19] can be stated as (6)–(9).

$$L_s \frac{di_{sq}}{dt} = -R_s i_{sq} - p L_s i_{sd} \Omega - \frac{2}{5} K_M \Omega + \frac{V_{dc}}{2} u_q \quad (6)$$

$$L_s \frac{di_{sd}}{dt} = -R_s i_{sd} + p i_{sq} \Omega + \frac{V_{dc}}{2} u_d \quad (7)$$

$$L_s \frac{di_{sx}}{dt} = -R_s i_{sx} + \frac{V_{dc}}{2} u_x \quad (8)$$

$$L_s \frac{di_{sy}}{dt} = -R_s i_{sy} + \frac{V_{dc}}{2} u_y \quad (9)$$

The variables $u_d, u_q, u_x,$ and u_y indicate the input signals control's average values of $(s_1, s_2, s_3, s_4, s_5)$. V_{dc} denotes the output voltage of the Vienna rectifier. The Vienna output voltage V_{dc} , can be expressed as (10).

$$C \frac{dV_{dc}}{dt} = \frac{5}{2} (u_d i_{sd} + u_q i_{sq} + u_x i_x + u_y i_y) - 2i_{ld} \quad (10)$$

Let us define the following state variables for convenience: $[x_1, x_2, x_3, x_4, x_5]^T = [\Omega, i_{sq}, i_{sd}, i_x, i_y]^T$. With this notation, by performing transformations on the system model equation, we can derive a state-space representation of the subsystem, which encompasses both the Vienna rectifier and the PMSG. The model can

be rewritten as (11)–(15):

$$\dot{x}_1 = -\frac{F}{J}x_1 + \frac{K_M}{J}x_2 - \frac{1}{J}T_g \quad (11)$$

$$\dot{x}_2 = -\frac{R_s}{L_s}x_2 - px_1x_3 - \frac{2}{5L_s}K_Mx_1 + \frac{V_{dc}}{2L_s}u_q \quad (12)$$

$$\dot{x}_3 = -\frac{R_s}{L_s}x_3 + px_1x_2 + \frac{V_{dc}}{2L_s}u_d \quad (13)$$

$$\dot{x}_4 = -\frac{R_s}{L_s}x_4 + \frac{V_{dc}}{2L_s}u_x \quad (14)$$

$$\dot{x}_5 = -\frac{R_s}{L_s}x_5 + \frac{V_{dc}}{2L_s}u_y \quad (15)$$

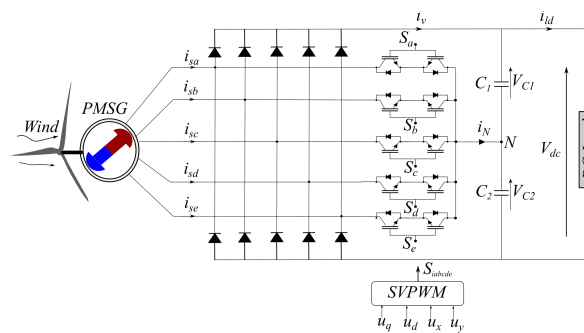


Figure 1. Electrical scheme of a five-phase PMSG with Vienna-type rectifier topology

3. WIND TURBINE CONTROLLER DESIGN

3.1. Control objectives

The work presented in this study aims to accomplish three primary objectives:

- Apply an electrical parameter-based neural network optimizer to extract the maximum power from wind speed.
- Improving the performance of the five-phase PMSG by regulating the stator machine currents, specifically i_{sd} , i_{sx} , and i_{sy} , to zero, as discussed in [20].
- Maintain voltage equilibrium at Vienna rectifier output and cancel neutral current [21], [22].

3.2. Space vector pulse width modulation

SVPWM is a sophisticated control technique extensively used for five-phase PMSGs. It involves dynamically modulating five distinct voltage vectors to generate precise sinusoidal voltage waveforms, optimizing power generation, reducing harmonics, and improving overall system performance. SVPWM plays a crucial role in maximizing energy conversion efficiency and promoting the adoption of renewable energy sources. This approach generates the output waveform using voltage vectors, which span ten sectors with 32 states each [23], [24]. Refer to Figure 2 for an overview of the fundamental notion of this strategy.

3.3. Wind turbine speed reference

The design of the speed optimizer utilizes advanced machine learning techniques. One key aspect of this design involves determining the reference speed, which plays a pivotal role in extracting the maximum power from the aerogenerator. Notably, this reference speed is established solely through electrical measurements. This emphasis on electrical parameters underscores the significance of precision in power extraction. The entire process is facilitated by an ANN, as visualized in Figure 3.

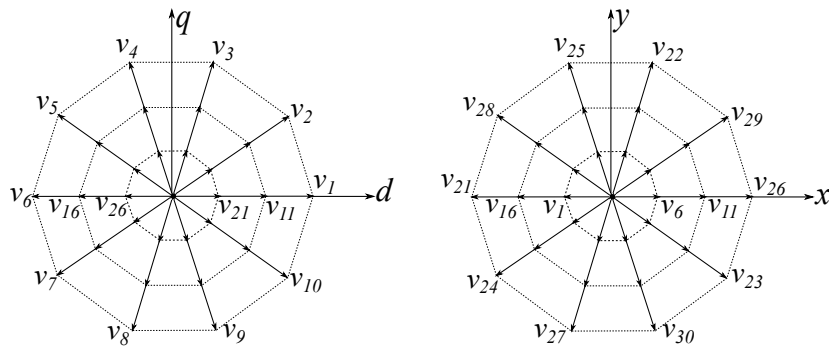


Figure 2. SPVWM in the dq and xy axes

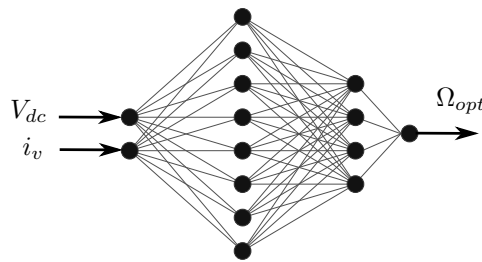


Figure 3. ANN speed optimizer

3.4. Speed regulation loop

The speed regulator is developed using the backstepping control technique, as described in the reference [25]. The speed error is defined as (16).

$$z_1 = x_1^* - x_1 \tag{16}$$

The expression for the time derivative of z_1 , denoted as \dot{z}_1 , can be written as (17).

$$\dot{z}_1 = \dot{x}_1^* + \frac{F}{J}x_1 - \frac{K_M}{J}x_2 + \frac{1}{J}T_g \tag{17}$$

Considering the quadrature Lyapunov function $V_1 = \frac{1}{2}z_1^2$. The dynamic of V_1 may be stated as (18).

$$\dot{V}_1 = z_1 \left(\dot{x}_1^* + \frac{F}{J}x_1 - \frac{K_M}{J}x_2 + \frac{1}{J}T_g \right) \tag{18}$$

Let use $\alpha = \frac{K_M}{J}x_2$ as a virtual input control for the z_1 -dynamics. The actual control inputs u_q indirectly influence z_1 through α . To get a stabilizing control law, we consider the quadrature Lyapunov function candidate $V_1 = \frac{1}{2}z_1^2$, the following virtual control α^* can be proposed as (19):

$$\alpha^* = \frac{F}{J}x_1 + \frac{1}{J}T_g + \dot{x}_1^* + k_1z_1 \tag{19}$$

k_1 presents a regulator gain.

Now, we proceed to design the current regulation loop for the quadratic component i_q and provide the control law signal u_q . We define the current error for the quadratic component as (20):

$$z_2 = \alpha^* - \alpha \tag{20}$$

Based on (19), it can be deduced from (17) that the dynamics of z_1 can be described by the (21).

$$\dot{z}_1 = -k_1z_1 + z_2 \tag{21}$$

To ensure asymptotic stability of the (z_1, z_2) error system, the next step involves determining the control input u_q . First, let's obtain the trajectory of the error z_2 . The expression for the dynamics of \dot{z}_2 is as (22):

$$\dot{z}_2 = \beta(x, t) - k_1^2 z_1 + k_1 z_2 - \frac{K_M}{2JL_s} u_q V_{dc} \quad (22)$$

where

$$\beta(x, t) = \frac{K_M}{J} \left(\frac{R_s}{L_s} x_2 + p x_1 x_3 + \frac{2K_M}{5L_s} x_1 \right) - \frac{F^2}{J^2} x_1 + \frac{FK_M}{J^2} x_2 - \frac{FT_g}{J^2} + \frac{\dot{T}_g}{J} - \ddot{x}_1^*$$

Let us consider the quadratic Lyapunov function candidate $V_2 = \frac{1}{2} z_1^2 + \frac{1}{2} z_2^2$. The time derivative of V_2 is:

$$\dot{V}_2 = -k_1 z_1^2 + z_1 z_2 + z_2 \dot{z}_2 \quad (23)$$

for the (z_1, z_2) -system to be globally asymptotically stable, it is sufficient to design the control u_q as (24):

$$\dot{V}_2 = -k_1 z_1^2 - k_2 z_2^2 \quad (24)$$

with k_2 being a design positive parameter, and the z_2 dynamic's is selected as (25):

$$\dot{z}_1 = -k_2 z_2 - z_1 \quad (25)$$

The input control law u_q , based on (22) can easily conclude that.

$$u_q = \frac{2JL_s}{K_M V_{dc}} \left((k_1 + k_2) z_2 - (k_1^2 - 1) z_1 + \beta(x, t) \right) \quad (26)$$

3.5. Five-phase PMSG current regulation

3.5.1. D-axis current regulation

We will now define the tracking error z_3 :

$$z_3 = x_3 - x_3^* = x_3 \quad (27)$$

to analyze the system stability, we use the quadratic Lyapunov function candidate $V_3 = \frac{1}{2} z_3^2$. The time derivative of V_3 is represented as (28).

$$\dot{V}_3 = z_3 \left(\frac{R_s}{L_s} x_3 - p x_1 x_2 - \frac{V_{dc}}{2L_s} u_d \right) \quad (28)$$

Based on (28) and considering the stabilizing Lyapunov condition, the control law u_d may be easily deduced as (29):

$$u_d = \frac{2L_s}{V_{dc}} \left(\frac{R_s}{L_s} x_3 - p x_2 x_1 + k_3 z_3 \right) \quad (29)$$

with k_3 is a design positive parameter.

3.5.2. Current control along XY-axis

As the xy-stator's current components demonstrate a comparable shape, the control law will share the same shape. Let's define the tracking error z_4 :

$$z_4 = x_4 - x_4^* = x_4 \quad (30)$$

let's consider the Lyapunov function candidate, $V_4 = \frac{1}{2} z_4^2$. The time derivative of V_4 can be expressed as (31).

$$\dot{V}_4 = z_4 \left(\frac{R_s}{L_s} x_4 - \frac{V_{dc}}{2L_s} u_x \right) \quad (31)$$

By considering the stabilizing Lyapunov condition and referring to (31), we can readily deduce the input control law u_x as (32).

$$u_x = \frac{2L_s}{V_{dc}} \left(\frac{R_s}{L_s} x_4 + k_4 z_4 \right) \quad (32)$$

The expression for the y-control law can be derived in the following manner:

$$u_y = \frac{2L_s}{V_{dc}} \left(\frac{R_s}{L_s} x_5 + k_5 z_5 \right) \quad (33)$$

with k_4 and k_5 being positive design parameters.

3.6. Simulation results

In this study, the electrical configuration comprises a five-phase aerogenerator linked to a Vienna AC/DC converter and subjected to an R-load, which may be considered an alternating current (AC) network, a storage battery system, or a direct current (DC) network. The performance of the designed controller was evaluated through a simulation using MATLAB/Simulink software. Figure 4 presents the simulation results, showcasing a variety of signals that reflect the performance of the adopted techniques. The purpose of this figure is to provide a comprehensive overview of the techniques' effectiveness. Figure 4(a) presents the chosen wind profile, and Figure 4(b) shows the rotor speeds. The signals of rotor speeds Ω and Ω_{ref} converge with a small excess, demonstrating the controller's successful extraction of the maximum power from the wind turbine. Figure 4(c) demonstrates another control objective, where the i_{sq} current, representing the machine's torque, undergoes variations in response to changes in wind speed while maintaining stability near zero. Moreover, the i_{sd} currents i_{sx} and i_{sy} remain at zero, as shown in Figure 4(d), aligning with the earlier established control objective. The simulation results in Figure 4(e) showcase the voltage through the Vienna rectifier's output capacitors. It is essential for the rectifier's output voltage to remain balanced, which is confirmed by the equality of V_{C1} and V_{C2} in the simulation results. This balance verifies the SVPWM controller method's efficiency. Furthermore, the Vienna output voltage V_{dc} is also presented. This voltage exhibits fluctuations corresponding to the rotor speed. It is worth noting that this study does not incorporate voltage regulation, which could be a separate focus for future research. The depicted control laws in Figure 4(f) illustrate the sinusoidal shape of the stator currents, showcasing a significant benefit of the Vienna rectifier with a low THD value.

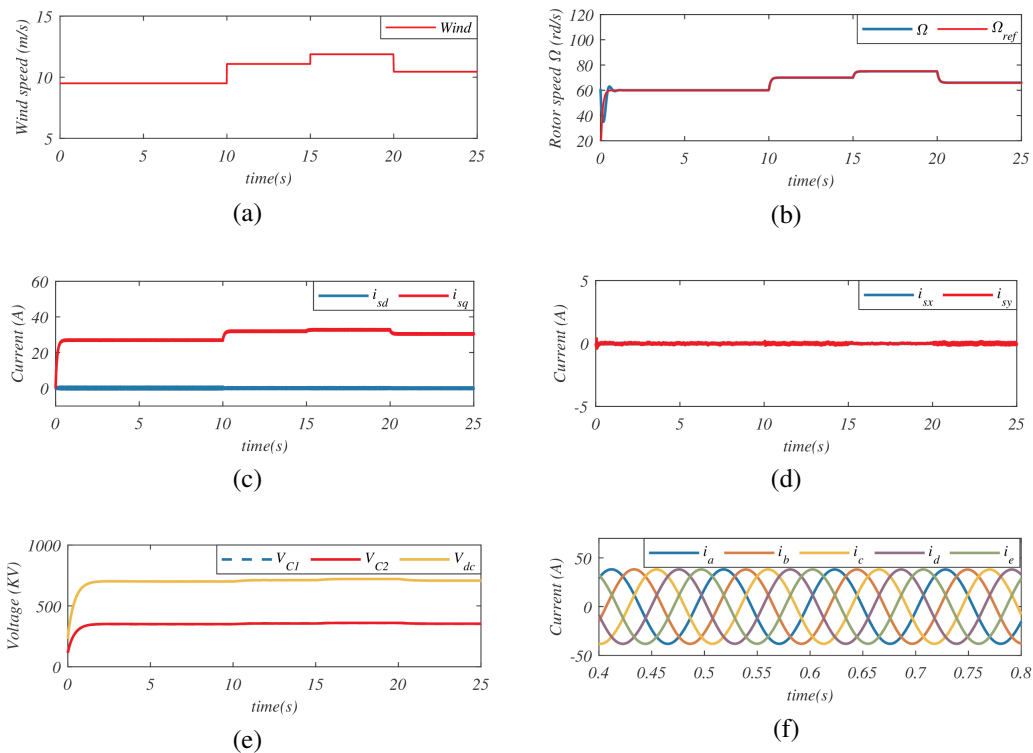


Figure 4. Simulation outcomes: (a) wind speed evolution, (b) Ω and Ω_{ref} , (c) stator current (i_{sd} , i_{sq}) (A), (d) stator current (i_{sx} , i_{sy}) (A), (e) capacitance voltage (V_{C1} , V_{C2}) and HVDC-line voltage V_{dc} (V), and (f) stator currents (A)

4. CONCLUSION

The integration of a five-phase aerogenerator, a Vienna AC/DC converter, and the SVPWM technique presents a viable solution for managing power flow in WECS. Through simulation results, it is evident that the backstepping controller and SVPWM work harmoniously to maintain a balanced voltage throughout the output

capacitors, maintaining a constant output voltage. Moreover, the incorporation of backstepping control for the five-phase machine has proven effective in achieving the desired control objectives. As a natural extension of this study, it would be worthwhile to investigate the overall system stability, encompassing the energy flow between these distinct entities.





REFERENCES

- [1] R. Ryndzionek, K. Blecharz, F. Kutt, M. Michna, and G. Kostro, "Fault-tolerant performance of the novel five-phase doubly-fed induction generator," *IEEE Access*, vol. 10, pp. 59350–59358, 2022, doi: 10.1109/ACCESS.2022.3179815.
- [2] A. Arafat, M. Z. Islam, M. T. Bin Tarek, and S. Choi, "Transient stability comparison between five-phase and three-phase permanent magnet assisted synchronous reluctance motor," in *2018 IEEE Transportation Electrification Conference and Expo (ITEC)*, Jun. 2018, pp. 1–6, doi: 10.1109/ITEC.2018.8450145.
- [3] T. A. Hussein and L. A. Mohammed, "Detailed Simulink implementation for induction motor control based on space vector pulse width modulation SVPWM," *Indonesian Journal of Electrical Engineering and Computer Science (IJECS)*, vol. 22, no. 3, pp. 1251–1262, Jun. 2021, doi: 10.11591/ijeecs.v22.i3.pp1251-1262.
- [4] V. Jayakumar, B. Chokkalingam, and J. L. Munda, "A comprehensive review on space vector modulation techniques for neutral point clamped multi-level inverters," *IEEE Access*, vol. 9, pp. 112104–112144, 2021, doi: 10.1109/ACCESS.2021.3100346.
- [5] S. Khadija, E. M. Ouadia, and F. Abdelmajid, "Nonlinear backstepping control of a partially shaded photovoltaic storage system," *Indonesian Journal of Electrical Engineering and Computer Science (IJECS)*, vol. 29, no. 1, pp. 225–237, Jan. 2022, doi: 10.11591/ijeecs.v29.i1.pp225-237.
- [6] Y. E. Mourabit, A. Derouich, A. E. Ghzizal, N. E. Ouanjli, and O. Zamzoum, "Nonlinear backstepping control for PMSG wind turbine used on the real wind profile of the Dakhla-Morocco city," *International Transactions on Electrical Energy Systems*, vol. 30, no. 4, Apr. 2020, doi: 10.1002/2050-7038.12297.
- [7] T. K. Roy, M. A. Mahmud, S. N. Islam, and A. M. T. Oo, "Nonlinear adaptive backstepping controller design for permanent magnet synchronous generator (PMSG)-based wind farms to enhance fault ride through capabilities," in *2019 IEEE Power & Energy Society General Meeting (PESGM)*, Aug. 2019, pp. 1–5, doi: 10.1109/PESGM40551.2019.8973758.
- [8] M. I. Berbek and A. A. Oglah, "Adaptive neuro-fuzzy controller trained by genetic-particle swarm for active queue management in internet congestion," *Indonesian Journal of Electrical Engineering and Computer Science (IJECS)*, vol. 26, no. 1, pp. 229–242, Apr. 2022, doi: 10.11591/ijeecs.v26.i1.pp229-242.
- [9] I. E. Myasse *et al.*, "Robust Nonlinear control design of MMC-HVDC systems for wind power plants integration," in *2023 3rd International Conference on Innovative Research in Applied Science, Engineering and Technology (IRASET)*, May 2023, pp. 1–5, doi: 10.1109/IRASET57153.2023.10152899.
- [10] S. Zou, J. Song, and O. Abdelkhalik, "A sliding mode control for wave energy converters in presence of unknown noise and nonlinearities," *Renewable Energy*, vol. 202, pp. 432–441, Jan. 2023, doi: 10.1016/j.renene.2022.11.078.
- [11] C. Liu and Y. Liu, "Adaptive finite-time stabilization for uncertain nonlinear systems with unknown control coefficients," *Automatica*, vol. 149, p. 110845, Mar. 2023, doi: 10.1016/j.automatica.2022.110845.
- [12] J. Pande, P. Nasikkar, K. Kotecha, and V. Varadarajan, "A review of maximum power point tracking algorithms for wind energy conversion systems," *Journal of Marine Science and Engineering*, vol. 9, no. 11, p. 1187, Oct. 2021, doi: 10.3390/jmse9111187.
- [13] A. Watil, A. E. Magri, R. Lajouad, A. Raihani, and F. Giri, "Multi-mode control strategy for a stand-alone wind energy conversion system with battery energy storage," *Journal of Energy Storage*, vol. 51, p. 104481, Jul. 2022, doi: 10.1016/j.est.2022.104481.
- [14] C. Jiang, H. Zhu, and X. Wang, "Decoupling control of outer rotor coreless bearingless permanent magnet synchronous generator based on fuzzy neural network inverse system," *IEEE Transactions on Transportation Electrification*, pp. 1–1, 2023, doi: 10.1109/TTE.2023.3253544.
- [15] N. F. Fadza'il, S. M. Zali, M. A. Khairudin, and N. H. Hanafi, "Stator winding fault detection of induction generator based wind turbine using ANN," *Indonesian Journal of Electrical Engineering and Computer Science (IJECS)*, vol. 19, no. 1, pp. 126–133, Jul. 2020, doi: 10.11591/ijeecs.v19.i1.pp126-133.
- [16] A. Watil, A. E. Magri, A. Raihani, R. Lajouad, and F. Giri, "An adaptive nonlinear observer for sensorless wind energy conversion system with PMSG," *Control Engineering Practice*, vol. 98, p. 104356, May 2020, doi: 10.1016/j.conengprac.2020.104356.
- [17] Z. Li, Y. Du, W. Zhao, T. Tao, and W. Tian, "Zero-sequence current suppression strategy for five-phase OW-PMSM with reduced common-mode voltage and inverter losses," *IEEE Transactions on Power Electronics*, vol. 38, no. 8, pp. 10116–10127, Aug. 2023, doi: 10.1109/TPEL.2023.3278317.
- [18] R. R. Kumar *et al.*, "Design and characteristics investigation of novel dual stator pseudo-pole five-phase permanent magnet synchronous generator for wind power application," *IEEE Access*, vol. 8, pp. 175788–175804, 2020, doi: 10.1109/ACCESS.2020.3025842.
- [19] A. Mansouri, A. E. Magri, R. Lajouad, F. Giri, and A. Watil, "An adaptive non-linear control of a wind energy conversion system connected to an HVDC line involving a Vienna rectifier," *IFAC-PapersOnLine*, vol. 55, no. 12, pp. 806–811, 2022, doi: 10.1016/j.ifacol.2022.07.412.
- [20] J. Deng, K. Shi, M. Chen, and D. Xu, "Analysis and design of zero-voltage-switching multiphase AC/DC converters," *IEEE Journal of Emerging and Selected Topics in Power Electronics*, vol. 10, no. 6, pp. 6495–6510, Dec. 2022, doi: 10.1109/JESTPE.2021.3129322.
- [21] L. Zhang *et al.*, "A modified DPWM with neutral point voltage balance capability for three-phase Vienna rectifiers," *IEEE Transactions on Power Electronics*, vol. 36, no. 1, pp. 263–273, Jan. 2021, doi: 10.1109/TPEL.2020.3002660.
- [22] Y. Zou *et al.*, "Dynamic-space-vector discontinuous PWM for three-phase Vienna rectifiers with unbalanced neutral-point voltage," *IEEE Transactions on Power Electronics*, vol. 36, no. 8, pp. 9015–9026, Aug. 2021, doi: 10.1109/TPEL.2021.3057120.
- [23] Q. Chen, L. Gu, Z. Lin, and G. Liu, "Extension of space-vector-signal-injection-based MTPA control into SVPWM fault-tolerant operation for five-phase IPMSM," *IEEE Transactions on Industrial Electronics*, vol. 67, no. 9, pp. 7321–7333, Sep. 2020, doi: 10.1109/TIE.2019.2944066.




- [24] U. R. Muduli, B. Chikondra, and R. K. Behera, "Space vector PWM based DTC scheme with reduced common mode voltage for five-phase induction motor drive," *IEEE Transactions on Power Electronics*, vol. 37, no. 1, pp. 114–124, Jan. 2022, doi: 10.1109/TPEL.2021.3092259.
- [25] I. E. Myasse *et al.*, "Observer and nonlinear control design of VSC-HVDC transmission system," *International Journal of Electrical Power & Energy Systems*, vol. 145, p. 108609, Feb. 2023, doi: 10.1016/j.ijepes.2022.108609.

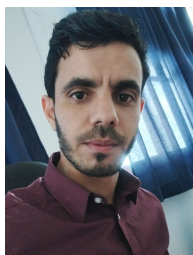
BIOGRAPHIES OF AUTHORS







Adil Mansouri     Ph.D. student Université Hassan II de Casablanca, Department of Electrical Engineering. Currently an electrical engineering professor in preparatory engineering classes. His research interests include optimization, observation and nonlinear control of AC machines, and renewable energy. He can be contacted at email: mansouri_adil@yahoo.com.







Abdelmounime El Magri    received his Ph.D. in electrical engineering - automatic control from Université de Mohammed V, Rabat, Morocco, in 2011. He is currently a professor at the Hassan II University, Casablanca Morocco. His research interests include optimization, observation and nonlinear control of AC machines, and energy conversion systems. He has coauthored several papers on these topics. He can be contacted at email: magri_mounaim@yahoo.fr.




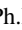


Ilyass El Myasse     Ph.D. student Université Hassan II de Casablanca, Department of Electrical Engineering. His research interests include optimization, observation and nonlinear control of AC machines, and renewable energy. He can be contacted at email: ilyaselmyasse@gmail.com.



Rachid Lajouad     was born in 1974. He received Ph.D. degree in electrical engineering from Mohammed V University, Rabat, Morocco, in 2016. Currently, he is a professor at the Hassan II University, Casablanca, Morocco. His research interests include optimization, observation and nonlinear control of AC machines, and renewable energy. He has published several journal/conference papers on these topics. He can be contacted at email: dsa.lajouad@gmail.com.



Nabil Elaadouli     Ph.D. student Université Hassan II de Casablanca, Department of Electrical Engineering. Currently an electrical engineering professor. His research interests include optimization, observation and nonlinear control of AC machines, and renewable energy. He can be contacted at email: n.elaadouli@gmail.com.